ELSEVIER

Biochemical Pharmacology 63 (2002) 733–743

Biochemical Pharmacology

Variation in the kinetics of caspase-3 activation, Bcl-2 phosphorylation and apoptotic morphology in unselected human ovarian cancer cell lines as a response to docetaxel

Geertruida M. Kolfschoten, Theresia M. Hulscher, Monique C.A. Duyndam, Herbert M. Pinedo, Epie Boven*

Department of Medical Oncology, Vrije Universiteit Medical Centre, Amsterdam, The Netherlands

Received 5 April 2001; accepted 30 October 2001

Abstract

Paclitaxel is able to cause cell death through the induction of apoptosis. Cell death characteristics for docetaxel have not yet been described in detail. We investigated four unselected human ovarian cancer cell lines for the sensitivity to a 1 hr exposure to docetaxel and calculated the concentrations inhibiting 50% (IC_{50}) and 90% (IC_{90}) of cell growth. Of the cell lines A2780, H134, IGROV-1 (all wild-type p53) and OVCAR-3 (mutant, mt p53) A2780 was most sensitive and OVCAR-3 least sensitive. Equitoxic drug concentrations representing IC_{90} values (25–510 nM) were applied for 1 hr to measure cell cycle distribution, DNA degradation, and to count apoptotic cell bodies and cells with multifragmented nuclei at various time-points after drug exposure. H134, IGROV-1 and OVCAR-3 showed a continued mitotic block up to at least 72 hr and prolonged presence of cells with multifragmented nuclei. High percentages of apoptosis were calculated at 48 hr and at later time-points. In contrast, A2780 cells accumulated in the S-phase of the cell cycle and apoptosis was hardly present. The changes in the expression levels of p53, p21/WAF1, Bax and Bcl-2, were not predictive for docetaxel-induced apoptosis. Caspase-3 activation occurred only in cells with accumulation in the G2/M phase starting as early as 8 hr in OVCAR-3. Prolonged Bcl-2 phosphorylation was evident in OVCAR-3, visible at 24 hr in H134 and IGROV-1, while this phenomenon did not occur in A2780. The mitogen-activated protein kinase pathway (JNKs/SAPKs or c-Jun N-terminal kinases/stress-activated protein kinases, JNK1/2; extracellular response kinase, ERK1/2; p38) did not seem to be directly involved in Bcl-2 phosphorylation or apoptosis. We conclude that docetaxel is able to activate caspase-3, induce Bcl-2 phosphorylation and apoptosis in cells that show a prolonged G2/M arrest, but cells may also die by a caspase-3-independent cell death mechanism.

Keywords: Docetaxel; Apoptosis; Human ovarian cancer cells; Caspase-3; Bax; Bcl-2

1. Introduction

The taxanes, docetaxel (Taxotere®) and paclitaxel (Taxol®), are anticancer agents effective in the treatment of multiple tumor types, including ovarian cancer [1]. Upon entering of a cancer cell into mitosis both drugs will promote the polymerization and inhibit the depolymerization of microtubules causing a mitotic arrest [2]. The ability to induce programmed cell death or apoptosis has been described mainly for paclitaxel, but not in detail for docetaxel.

The biochemical events leading to apoptosis by taxanes are still not well understood. It has been demonstrated that paclitaxel concentrations resulting in at least 50% cell death, inhibit mitosis in metaphase by stabilizing microtubule dynamics instead of altering microtubule polymer mass [3]. After removal of the drug, cells exited into an apparent interphase multinuclear state, which finally resulted in apoptosis. Apart from a G2/M arrest, paclitaxel-induced apoptosis can also be initiated in the S-phase of the cell cycle [4].

Several apoptosis-related proteins can be involved in the induction of programmed cell death. The expression of both tumor suppressor proteins p53 and p21/WAF1 can be

* Corresponding author. Tel.: +31-20-444-4336; fax: +31-20-444-4355.
E-mail address: e.boven@vumc.nl (E. Boven).

Abbreviations: JNK1/2, JNKs/SAPKs or c-Jun N-terminal kinases/stress-activated protein kinases; MAPK, mitogen-associated protein kinase; ERK1/2, extracellular response kinase; wt, wild-type; mt, mutant; MTT, 3-(4,5-dimethylthiazol-2-yl)-2,6-dimethyl-morpholino)-2,5-diphenyl-tetrazolium bromide; PBS, phosphate-buffered saline; MGG, May–Grünwald Giemsa; AMC, 7-amino-4-methylcoumarin.

0006-2952/02/$ – see front matter
PII: S0006-2952(01)00895-4

upregulated upon treatment with paclitaxel [5–7]. Functional p53 is not required for paclitaxel-induced apoptosis [8,9]. Paclitaxel can induce accumulation of p21/WAF1 independent of the status of p53 [5]. Elevation of p21/WAF1 parallels the inhibition of $p34^{cdc2}$ activity, which is important in the transition of cells through the G2/M phase of the cell cycle [10]. The latter group has also demonstrated that the increase in p21/WAF1 followed mitotic arrest and it was suggested that it has a role to facilitate cells to exit from abnormal mitosis. p21/WAF1 is also an inhibitor of cdk2 and cdk4, which are both important in G1/S cell cycle progression.

Paclitaxel-induced mitotic arrest appears to precede cytosolic cytochrome *c*-mediated cleavage and activation of caspase-3 [11]. Caspase-3 has been reported to play a key role in apoptosis as inhibition of its activity in a number of tumor cells prevented apoptosis [12]. The Bcl-2 family members are involved in the regulation of apoptosis by either inhibiting (e.g. Bcl-2) or promoting apoptosis (e.g. Bax) [13]. The pro-apoptotic proteins stimulate the release of cytochrome *c* from the mitochondria, which results in the activation of caspase-3. Heterodimerization of Bcl-2 with Bax appears to be critical in preventing Bax-mediated apoptosis. Paclitaxel can upregulate Bax expression [14]. This compound can also induce Bcl-2 hyperphosphorylation resulting in decreased binding to Bax, which in turn decreases the Bcl-2/Bax ratio allowing Bax-mediated apoptosis [14]. Bcl-2 phosphorylation seems to occur only in cells blocked at the G2/M phase of the cell cycle [15,16]. Raf-1 activation by paclitaxel has been reported to coincide with Bcl-2 phosphorylation, as phosphorylation was abrogated in the absence of Raf-1 [17]. It appears that docetaxel is more potent in inducing Bcl-2 phosphorylation than paclitaxel [15].

JNK1/2, a subfamily of the mitogen-associated protein kinase (MAPK) superfamily, is frequently associated with apoptosis. JNK1/2 can be activated upon treatment with paclitaxel [18,19]. Activated JNK1/2 phosphorylates a variety of transcription factors, including c-Jun. In general, JNK1/2 activation occurs prior to caspase-3 activation [19,20]. A possible role for JNK1/2 in the phosphorylation of Bcl-2 has been suggested [21,22]. Others, however, have shown that JNK1/2 was not or indirectly involved in the phosphorylation of Bcl-2 [19,23]. The activity of other members of the MAPK superfamily, ERK1/2 and p38 can also be influenced by microtubule-targeting agents [20]. Blagosklonny *et al*. [24] has demonstrated that inhibition of the MAPK pathway does not abrogate Bcl-2 phosphorylation or apoptosis.

In this study, we determined the apoptotic behavior of four human ovarian cancer cell lines upon treatment with docetaxel. We investigated the cell cycle distribution, the extent of apoptosis, and the caspase-3 activity at several time-points after a 1 hr exposure to IC_{90} concentrations of docetaxel. In addition, we determined the role of multiple proteins, including p53, p21/WAF1, Bax and Bcl-2 in the apoptotic process. Bcl-2 phosphorylation and the impact of MAPKs on Bcl-2 phosphorylation were measured. The results on the kinetic expression or phosphorylation of the proteins were analyzed to understand their possible influence on the apoptotic process. We also report the finding that microtubule damage and apoptosis are not related to the sensitivity to equitoxic doses of docetaxel.

2. Materials and methods

2.1. Cell lines and drug sensitivity

Four human ovarian cancer cell lines: A2780, H134, IGROV-1 and OVCAR-3 were used [25]. The cell lines were grown in monolayer cultures in Dulbecco's modified Eagle's medium (Gibco) supplemented with 10% fetal calf serum (FCS; Harlan Sera-lab Ltd.), 50 IU/mL penicillin and 50 μg/mL streptomycin (ICN) in an incubator with a humidified atmosphere containing 5% CO_2. The p53 status of the cell lines was determined by the polymerase chain reaction and sequencing of exons 5–9. Our recent sequence analysis revealed that A2780, H134 and IGROV-1 express wt p53, while OVCAR-3 expresses mt p53 (mutation at codon 248) (data not shown). These results are in agreement with earlier data reported in A2780, IGROV-1 and OVCAR-3 [25].

The antiproliferative effect of docetaxel (Taxotere®; Rhône-Poulenc Rorer) was evaluated by means of the 3-(4,5-dimethylthiazol-2-yl)-(2,6-dimethyl-morpholino)-2,5-diphenyl-tetrazolium bromide (MTT) assay. In brief, single-cell suspensions were plated into 96-well plates and grown for 24 hr. Cells were exposed to varying concentrations of docetaxel for 1 hr, after which the drug was removed and cells were incubated for an additional 72 hr in drug-free medium. The extinction of each well was measured at a wavelength of 540 nm using a Labsystems Multiscan Bichromatic plate reader (Labsystems). Drug effects were expressed as the IC_{50} and IC_{90}, which are the concentrations of the drug inducing 50 and 90% inhibition of growth of treated cells when compared to control cell growth. All drug concentrations were tested in four replicate wells and the experiments were repeated at least four times.

2.2. Docetaxel treatment

In the following experiments, the four cell lines were treated with docetaxel in a similar fashion for 1 hr with their respective IC_{90} concentrations determined by the MTT assay as already described. After a 1 hr-exposure docetaxel was removed and replaced by drug-free medium. Cells were harvested at 0, 8, 24, 48, 72 and 96 hr after drug exposure, except for the study on the phosphorylation of the MAPKs. In all experiments both adherent cells and cells in the supernatant (nonadherent) were combined for analysis. Cells which were not treated were included as controls.

2.3. Cell cycle analysis and apoptosis

Cell cycle analysis and the measurement of the percentage of apoptotic cells were assessed by flow cytometry. In brief, cells were seeded onto T25 flasks and not treated or treated with IC_{50} or IC_{90} concentrations of docetaxel. At various time-points adherent and nonadherent cells were recovered, washed with phosphate-buffered saline (PBS), fixed in 70% ethanol and stored at 4° until use. Cells were dehydrated in PBS, incubated for 20 min at room temperature with 250 μg/mL RNAse A (Roche) with 0.1% Triton-X-100 (ICN) and 20 min at 4° with 50 μg/mL propidium iodide (ICN) in the dark. The cell cycle distribution and the percentage of apoptotic cells were determined with a FACScan flow cytometer, using Cellfit software for the cell cycle and LYSIS II software for the percentage of apoptosis (Becton Dickinson). The determination of the cell cycle distribution and the percentage of apoptosis was repeated three times.

2.4. Morphology

Adherent and nonadherent cells were recovered at various time-points after docetaxel treatment and cytospins were prepared. The cytospin preparations were rinsed with PBS and fixed in acetone. Nuclei were stained with May–Grünwald Giemsa (MGG) and the percentages of cells containing multifragmented or condensed nuclei were determined by light microscopy, counting at least 100 cells twice by two independent observers.

In situ end-labeling of fragmented DNA was performed by the TUNEL technique [26] on cytospin preparations. Cells were fixed for 10 min in 3% paraformaldehyde in PBS. The incorporation of fluorescein-dUTP (TUNEL Label Mix; Boehringer, Mannheim) was catalyzed by the enzyme terminal deoxynucleotidyl transferase (TdT). To determine the morphology of the nuclei, the slides were double stained with DAPI (Roche). After staining with TUNEL, the slides were washed with PBS and once with DAPI. Thereafter, slides were incubated with DAPI for 15 min at 37° and washed with methanol. Vectashield (Vector) was used as mounting medium and the slides were analyzed with the fluorescence microscope. The percentage of cells containing apoptotic nuclei was determined by counting at least 100 cells twice by two independent observers.

2.5. Caspase-3 activity

The activity of caspase-3-like proteases was measured as described before [27]. Adherent and nonadherent cells were recovered after docetaxel treatment and washed with PBS. The pellet was resuspended in lysis buffer containing 10 mM Tris–HCl pH 7.6, 150 mM NaCl, 5 mM EDTA and 1% Triton-X-100. After 3 cycles of freeze/thawing the samples were centrifuged for 10 min at 10,000 *g*. Protein concentrations were determined using the Coomassie Plus Protein assay (Pierce). A 10 μg sample of protein in a total volume of 20 μL was added to 80 μL of reaction buffer (100 mM HEPES pH 7.3, 10% (w/v) sucrose, 0.1% (v/v) Nonidet-P40, 10 mM DTT, and 25 μM of DEVD-7-amino-4-methylcoumarin (AMC) substrate (Sigma) in a white 96-wells plate (Costar). The fluorescence of the cleaved substrate was measured every 2 min for 45 min at 37° in a bioassay (Perkin-Elmer) at 360 nm excitation and 446 nm emission. To calculate the caspase-3 activity calibration curves were constructed using free AMC. The determination of the caspase-3 activity was carried out in two independent experiments.

2.6. Western blot

For Western blot analysis, adherent and nonadherent cells were washed with PBS and lysed in lysis buffer (10 mM Tris–HCl pH 7.6, 150 mM NaCl, 5 mM EDTA and 1% Triton-X-100) supplemented with the protease inhibitors phenylmethylsulphonyl fluoride (1 mM; Merck), leupeptin (10 μM; Sigma) and trypsin inhibitor (Sigma). Protein concentrations were determined using the Coomassie Plus Protein assay (Pierce).

A 25 μg (p53, Bcl-2 and Bax) or 50 μg of protein (p21/WAF1) were electrophoresed through a 12% SDS-polyacrylamide gel and transferred to Immobilon-P transfer membrane (Millipore). Membranes were blocked with 5% milk solution (Protifar; Nutricia) in PBS with 0.2% Tween-20. Blots were incubated for 1 hr at room temperature with specific monoclonal antibodies against p53 (DO-7; DAKO), p21/WAF1 (Ab-1; oncogene), and Bcl-2 (124; DAKO), or a polyclonal antibody against Bax (p19; DAKO).

For detection of the MAPKs, 50 μg of protein was loaded onto a 10% polyacrylamide gel and transferred to Immobilon-P transfer membrane. Blots were blocked in 5% milk solution and incubated overnight at 4° for staining with polyclonal antibodies against phospho JNK1/JNK2, phospho ERK1/2, phospho p38, phospho c-Jun (ser 63) and total JNK1/JNK2, ERK1/2, p38 and c-Jun (New England Biolabs).

Antibody binding was revealed by peroxidase secondary antibodies (DAKO and New England Biolabs) and visualized using enhanced chemiluminescence (Sigma). Quantification was carried out using Molecular Analyst Software (Biorad). Western blot analysis was carried out in two independent experiments.

3. Results

3.1. Sensitivity to docetaxel

Table 1 represents the IC_{50} and IC_{90} concentrations as calculated for the four human ovarian cancer cell lines after a 1 hr exposure to docetaxel, followed by a 72 hr drug-free exposure. A2780 was the most sensitive cell line, followed

Table 1
Sensitivity of human ovarian cancer cell lines after a 1 hr exposure to docetaxel and a 72 hr drug-free exposure as determined by the MTT assay

Cell line	IC_{50} mean in M (±SD)[a]	IC_{90} mean in M (±SD)[a]
A2780	2.8 (±0.7) × 10^{-9}	2.5 (±2.0) × 10^{-8}
H134	5.2 (±3.4) × 10^{-9}	2.0 (±1.4) × 10^{-7}
IGROV-1	8.7 (±8.4) × 10^{-8}	4.2 (±3.1) × 10^{-7}
OVCAR-3	5.1 (±3.6) × 10^{-8}	5.1 (±3.7) × 10^{-7}

[a] Mean values of at least four experiments.

by H134, IGROV-1 and OVCAR-3. The IC_{90} concentrations of A2780 and OVCAR-3 varied 20-fold.

In the next experiments, a control MTT assay was included to reconfirm the used IC_{50} and IC_{90} concentrations of docetaxel. For the data presented IC_{90} concentrations represented experiments in which growth inhibition (±SEM) was obtained for A2780 84 ± 5%, for H134 84 ± 7%, for IGROV-1 86 ± 7%, and for OVCAR-3 89 ± 6%. In three separate experiments the MTT assay was carried out at 0, 8, 24, 48, 72 hr after the 1 hr exposure to the individual IC_{90} concentrations of docetaxel. In all four cell lines growth in treated cells was suppressed to a similar extent confirming equitoxic drug treatment (data not shown).

3.2. Cell cycle analysis

Cells were treated for 1 hr with IC_{90} concentrations of docetaxel and both adherent and nonadherent cells were harvested at 0, 8, 24, 48 and 72 hr after removing the drug to determine the cell cycle distribution by FACS analysis. Docetaxel-induced reproducible changes and the results of a representative experiment are depicted in Fig. 1. The cell cycle distribution of the control cells hardly changed in time. After 48–72 hr, cells tended to accumulate in the G0/G1 phase of the cell cycle. In the docetaxel-treated cells, a change in the cell cycle distribution was most pronounced in H134, IGROV-1 and OVCAR-3 cells. Already after 8 hr cells started to accumulate in the G2/M phase of the cell cycle. This accumulation proceeded until 24 hr in OVCAR-3 cells and until 48 hr in H134 and IGROV-1 cells. The percentage of cells accumulating in the G2/M phase decreased slightly thereafter. In contrast, in A2780 an increase of cells in the S-phase was visible in time. After 48 hr, this accumulation was maximal and after 72 hr the cell cycle distribution was comparable to the cell cycle distribution of the control cells.

From this experiment it can be concluded that docetaxel is able to induce a G2/M arrest in H134 wt p53, IGROV-1 wt p53 and OVCAR-3 mt-p53 cells, but this is not observed in A2780 wt-p53 cells.

3.3. Evaluation of apoptosis

Three techniques were used to determine the percentage of apoptosis induced by docetaxel. Cells were treated with IC_{90} concentrations of docetaxel for 1 hr and harvested at 0, 8, 24, 48, 72 and 96 hr after exposure. The results are summarized in Fig. 2. The percentage of apoptosis in the control cells remained low in time in all cell lines. The results after treatment obtained with the three techniques did show differences in percentages, but overall, the patterns were in line for each cell line.

With FACS analysis, an increase in the number of cells with subG0 DNA content, representative for apoptotic cells, was measurable after 24 hr in H134, IGROV-1 and OVCAR-3 cells. The percentage of apoptotic IGROV-1 cells still increased till 28% at 96 hr and was highest, followed by OVCAR-3 (22%), H134 (18%) and A2780 (3%) cells.

MGG staining was used to visualize nuclear changes and showed numerous mitotic cell figures in H134, IGROV-1 and OVCAR-3 cells at 24 hr. The percentage of mitotic cells was highest in OVCAR-3 (45%) at 24 hr after treatment. At 24 hr multifragmented nuclei appeared among H134, IGROV-1 and OVCAR-3 cells. OVCAR-3 cells showed the highest percentage of multifragmented nuclei (78%) at 48 hr. The percentage of cells with condensed nuclei representing apoptotic cells increased first in IGROV-1 cells after 24 hr, followed by OVCAR-3, H134 and A2780 cells after 48 hr. At 96 hr, the percentage was highest in OVCAR-3 cells (65%), followed by IGROV-1 (39%), H134 (32%) and A2780 (6%) cells.

TUNEL staining was performed in a separate experiment to determine if the cells with multifragmented nuclei were apoptotic. Slides were double-stained with DAPI to distinguish the morphology of the nucleus. Again, the increase in apoptosis was earliest in IGROV-1 cells and maximal (60%) at 48 hr. At 96 hr, the percentage of apoptosis was highest in OVCAR-3 (73%), followed by H134 (68%), IGROV-1 (51%) and A2780 (7%) cells. Of interest, cells with multifragmented nuclei initially stained negative with TUNEL. At 72 and 96 hr, a proportion of the multifragmented nuclei stained with TUNEL. DAPI staining at 96 hr in both H134 and IGROV-1 revealed that 96% of cells showed multiple nucleic fragments, while the percentage was 63% in OVCAR-3 and 0% in A2780.

This experiment indicates that the extent of apoptosis induced by docetaxel is not related to the sensitivity of the cells. Furthermore, apoptosis is independent of the p53 status. Cells in mitotic arrest are progressing to cells with multifragmented nuclei that can be visualized from 24 hr until at least 96 hr after treatment. Cells with multifragmented nuclei at early time-points do not show positive TUNEL staining. At later time-points, however, a proportion of cells with multifragmented nuclei stain positive for TUNEL. TUNEL and to a lesser extent also MGG staining, indicate a higher percentage of cells with apoptotic features than measured by FACS.

3.4. Caspase-3 activity

The conversion of the substrate DEVD-AMC into free AMC was used as a measure of caspase-3 activity upon

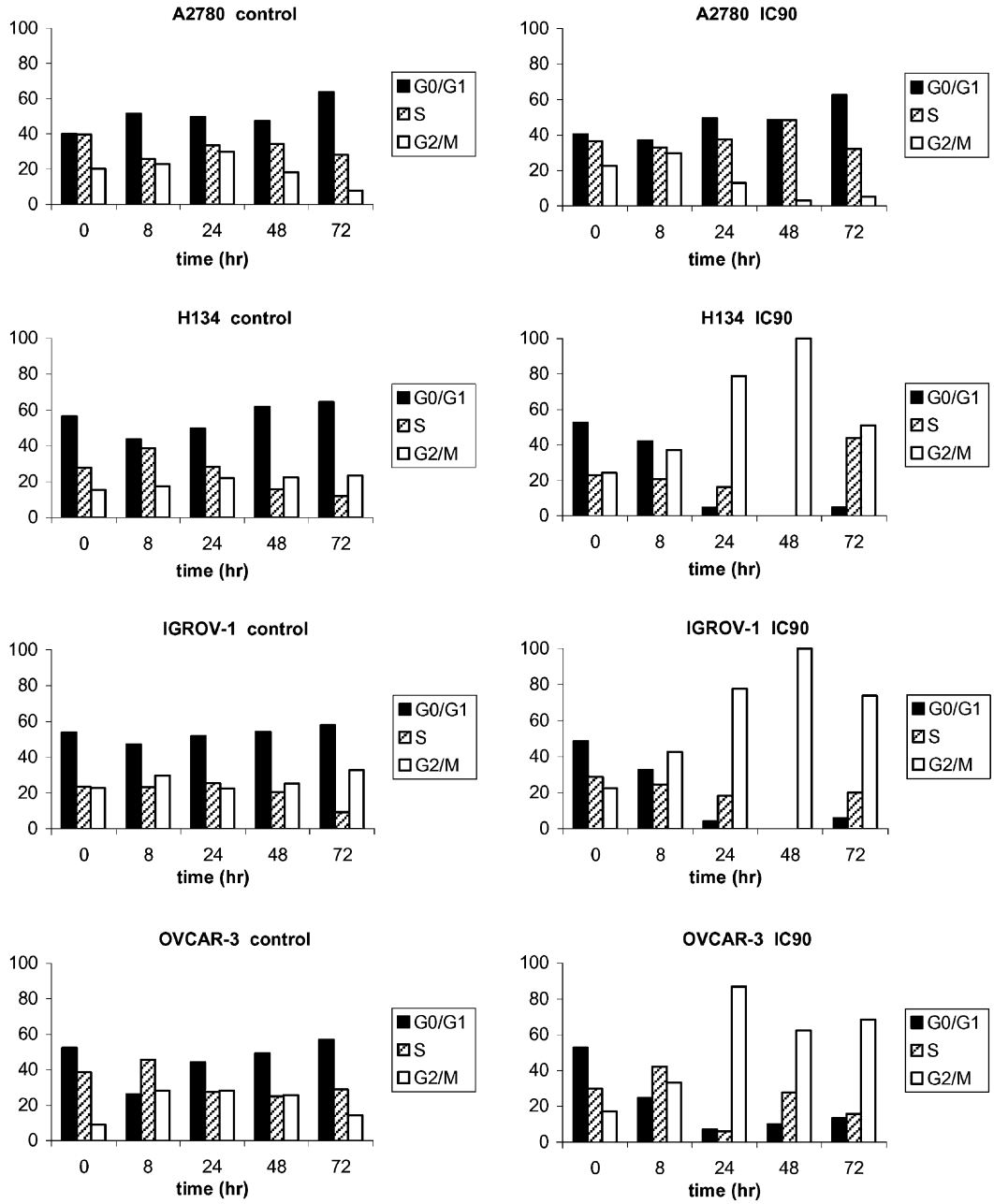

Fig. 1. The cell cycle distribution determined by FACS analysis and expressed in percentages. A2780, H134, IGROV-1 and OVCAR-3 cells were not treated (control) or treated with IC_{90} concentrations of docetaxel. The cells were harvested at 0, 8, 24, 48 and 72 hr after a 1 hr exposure.

treatment with IC_{90} concentrations of docetaxel (Fig. 3). Caspase-3 activity increased first in OVCAR-3 cells at 8 hr and was highest at 96 hr. At 48 hr, activity was maximal in IGROV-1 cells and decreased thereafter. The caspase-3 activity in H134 cells only showed a slight increase and it remained low in A2780 cells at all time-points measured.

Overall, caspase-3 activity in the cells seems to increase at the same time-points (OVCAR-3) or slightly later (H134, IGROV-1) than the accumulation of cells in the G2/M phase, which is already visible at 8 hr. The increase in caspase-3 activity precedes DNA degradation and nuclear changes. In A2780 cells, apoptosis is less than 10% and caspase-3, as expected, is hardly affected.

3.5. Apoptosis-related proteins

Our earlier results indicated that the constitutive expression levels of the proteins varied among the cell lines in a comparative experiment (data not shown). As expected, the constitutive level of p53 was highest in the mt p53 OVCAR-3 cell line. The constitutive p21/WAF1 expression was highest in IGROV-1 cells. Similar expression levels of the pro-apoptotic protein Bax were noted in the

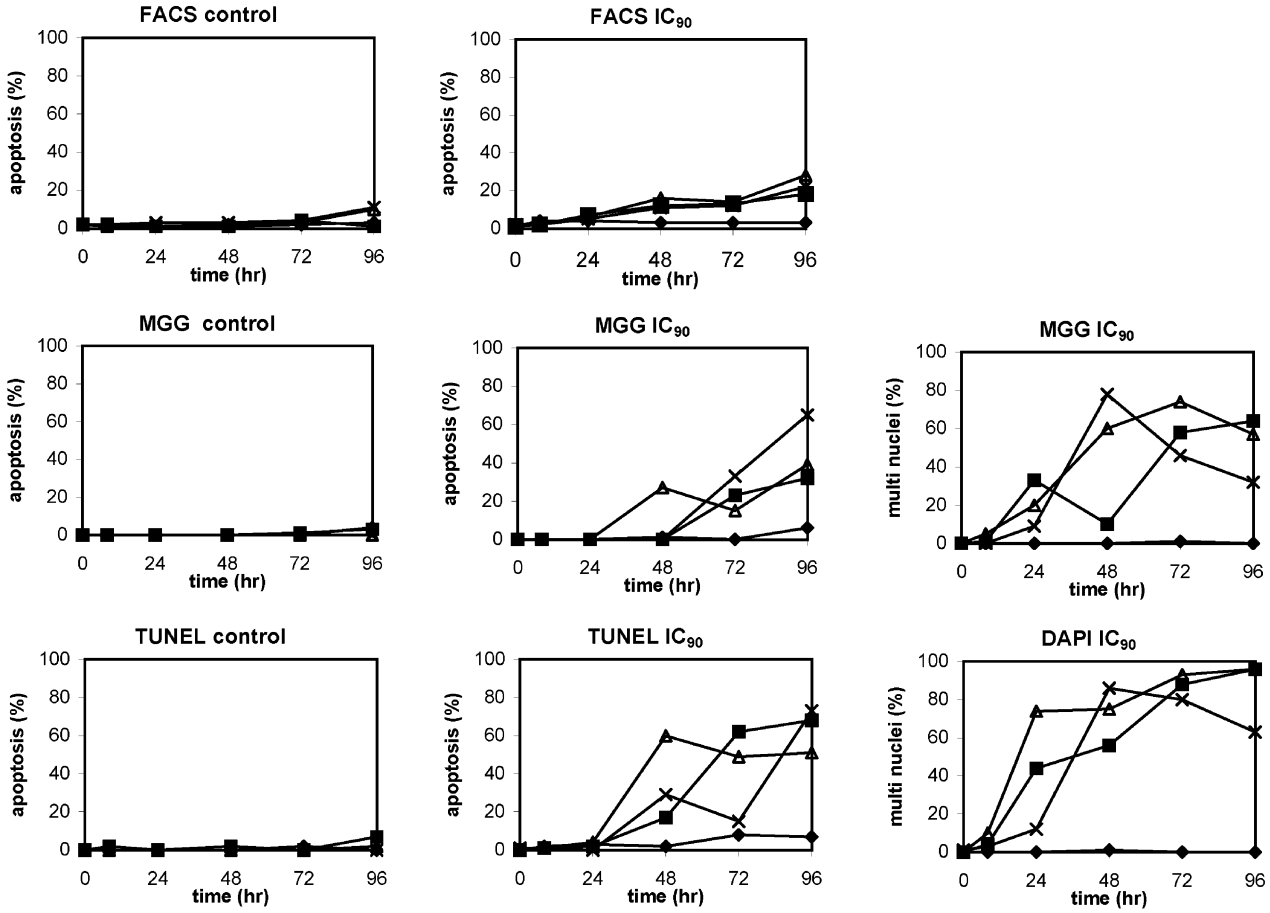

Fig. 2. The percentage of apoptosis determined by FACS analysis, MGG and TUNEL staining. In addition, cells with multifragmented nuclei were counted by MGG and DAPI staining. A2780 (◆), H134 (■), IGROV-1 (△) and OVCAR-3 (×) cells were treated with IC_{90} concentrations of docetaxel. Cells were harvested at 0, 8, 24, 48, 72 and 96 hr after a 1 hr drug exposure. The values given for FACS are the mean of four experiments. For MGG and TUNEL/DAPI two independent observers counted at least 100 cells in each experiment.

four cell lines. For the Bcl-2, anti-apoptotic protein the expression level was highest in OVCAR-3, and not detectable in A2780.

The expression levels of p53, p21/WAF1, Bax and Bcl-2 at several time-points after the 1 hr exposure to IC_{90} concentrations of docetaxel, relative to the expression levels in control samples at the same time-points are depicted in Table 2. Overall, no pronounced changes were observed in the expression levels of the proteins in the control samples at the various time-points measured. The expression levels of p53 increased 3.8-, 5.4-, and 2.9-fold in, respectively, A2780, H134, and IGROV-1, but not in OVCAR-3 expressing mt p53. The expression levels of p21/WAF1 only increased in the cell lines expressing wt p53. The 6.9-fold increase was maximal at 8 hr in A2780 and decreased gradually. Maximal p21/WAF1 upregulation occurred at

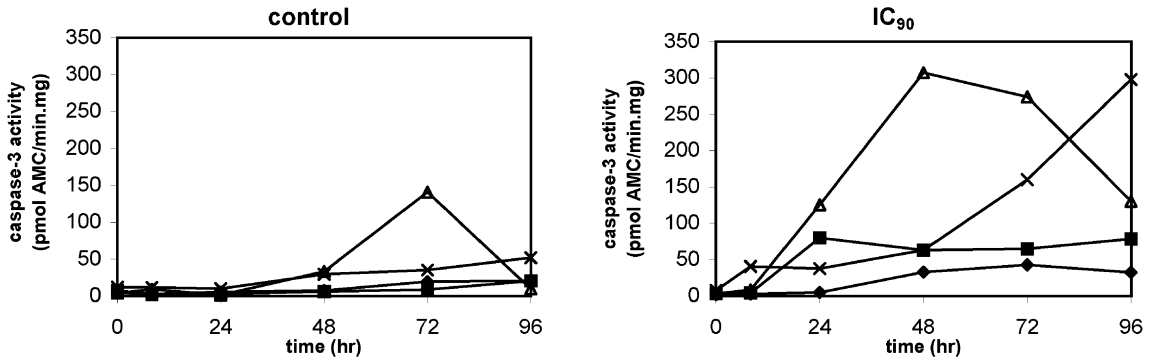

Fig. 3. Caspase-3 activity expressed as pico molar liberated AMC/min mg protein in control A2780 (◆), H134 (■), IGROV-1 (△) and OVCAR-3 (×) and in cells after treatment with IC_{90} concentrations of docetaxel. The cells were harvested at 0, 8, 24, 48, 72 and 96 hr after a 1 hr drug exposure. The values are the mean of two independent experiments.

Table 2
The induction of apoptosis-related proteins in A2780, H134, IGROV-1 and OVCAR-3 cells upon treatment with docetaxel

Cell line	Time-point (hr)	p53	p21/WAF1	Bax	Bcl-2
A2780	0	0.8	0.7	0.9	n.d.
	8	3.8	6.9	1.6	n.d.
	24	3.6	4.8	2.8	n.d.
	48	2.8	3.0	3.7	n.d.
	72	3.3	1.5	3.4	n.d.
H134	0	1.0	1.2	1.2	0.9
	8	1.4	1.3	0.9	1.2
	24	1.9	2.7	0.5	1.3
	48	5.1	3.1	0.9	0.6
	72	5.4	2.3	1.6	0.7
IGROV-1	0	1.0	1.0	1.4	1.4
	8	1.4	2.2	1.1	1.0
	24	1.2	4.4	1.1	1.3
	48	1.7	4.4	0.7	1.9
	72	2.9	7.6	0.8	1.6
OVCAR-3	0	1.7	0.8	2.6	2.3
	8	1.1	0.5	2.7	1.0
	24	0.9	0.6	4.1	2.5
	48	0.7	0.6	2.0	2.2
	72	1.0	0.5	0.8	1.3

The protein expression levels of p53, p21/WAF1, Bax and Bcl-2 after a 1 hr exposure to IC_{90} concentrations of docetaxel, relative to the expression levels in control cells at the same time-points. Cells were harvested 0, 8, 24, 48 and 72 hr after treatment, lysed and protein samples (25 μg for p53, Bax and Bcl-2; 50 μg for p21/WAF1) were separated by SDS-PAGE. Similar exposure times were used for the visualization of each protein. The results are the mean of two independent experiments. n.d.: not detectable.

48 hr in H134 (3.1-fold) and at 72 hr in IGROV-1 cells (7.6-fold). In A2780, Bax expression increased in time, while in H134 and IGROV-1 changes were not pronounced. In OVCAR-3, slightly elevated Bax expression levels after treatment decreased in time. Bcl-2 expression levels were not detectable in A2780 under the conditions used for the experiments and this did not change upon treatment with docetaxel. Except for a slight increase in OVCAR-3, no pronounced changes in Bcl-2 were detected in the other cell lines.

Although an increase in p53 and p21/WAF1 expression was detected in the cell lines containing wt p53, no relation was found between the expression levels and the apoptotic behavior of the cells. A G2/M arrest could occur independently of an increase in either p53 or p21/WAF1 as shown for OVCAR-3 cells. In contrast, p21/WAF1 upregulation in A2780 did not result in a G2/M arrest. Furthermore, the increase in the expression levels of Bax in A2780 did not result in a high number of apoptotic cells. Overall, slight changes in Bax or Bcl-2 were not indicative for the clear apoptotic features in the other three cell lines.

3.6. Bcl-2 phosphorylation

The Bcl-2 phosphorylation status was determined in the cell lines at 0, 8, 24, 48, 72 and 96 hr after a 1 hr treatment with docetaxel (Fig. 4). Bcl-2 was already phosphorylated at 8 hr in the OVCAR-3 cells, which reached a maximum at 24 hr and remained visible until at least 96 hr. In H134 and IGROV-1, phosphorylation was detectable at 24 hr and was no longer detectable after that in H134, while a slight phosphorylation was still visible in IGROV-1. Bcl-2 was only detectable in A2780 cells using a long exposure time, but phosphorylation was absent.

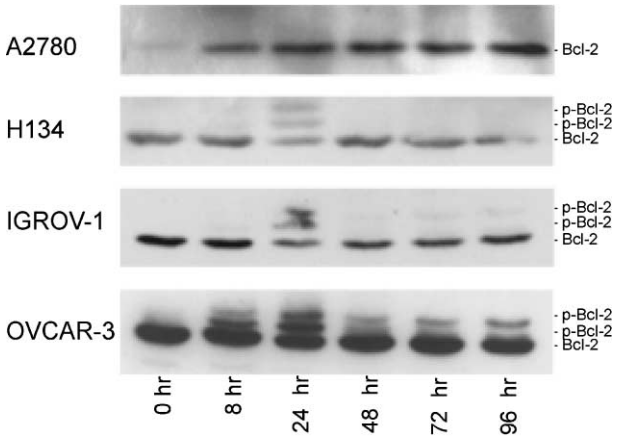

Fig. 4. Bcl-2 phosphorylation in A2780, H134, IGROV-1 and OVCAR-3. Cells were treated with IC_{90} concentrations of docetaxel and harvested at 0, 8, 24, 48, 72, and 96 hr after a 1 hr drug exposure. Protein samples (50 μg) were analyzed by Western blot. For A2780 a longer time period was used to visualize Bcl-2.

It thus appears, that Bcl-2 phosphorylation only occurs in cells with a G2/M arrest. The duration of Bcl-2 phosphorylation, however, does not relate to the extent of apoptosis.

3.7. Mitogen-activated protein kinases

Conflicting data have been reported about the role of MAPKs, and in particular of JNK1/2, in Bcl-2 phosphorylation. Furthermore, MAPKs are frequently associated with apoptosis. Therefore, we determined the phosphorylation of ERK1/2, JNK1/2 and p38 upon treatment with docetaxel. Earlier time-points were chosen in this experiment, since it has been described that docetaxel induces a transient activation of the MAPKs [20]. Samples of cells treated for 4 hr with arsenite (100 μM) were included as a positive control [28].

Although the expression levels of ERK1/2 varied between the cell lines, in H134, IGROV-1 and OVCAR-3 no difference in the phosphorylation status could be detected between treated and control samples. As an example, the results obtained with OVCAR-3 cells upon treatment with docetaxel are depicted in Fig. 5A. In A2780, the phosphorylated ERK1/2 level was slightly higher in the treated samples, which was best visible at 3 hr after the docetaxel exposure (Fig. 5A). The levels of total ERK1/2 remained similar in time.

In A2780 and OVCAR-3 low levels of phosphorylated p38 were detectable, but the levels in treated cells remained

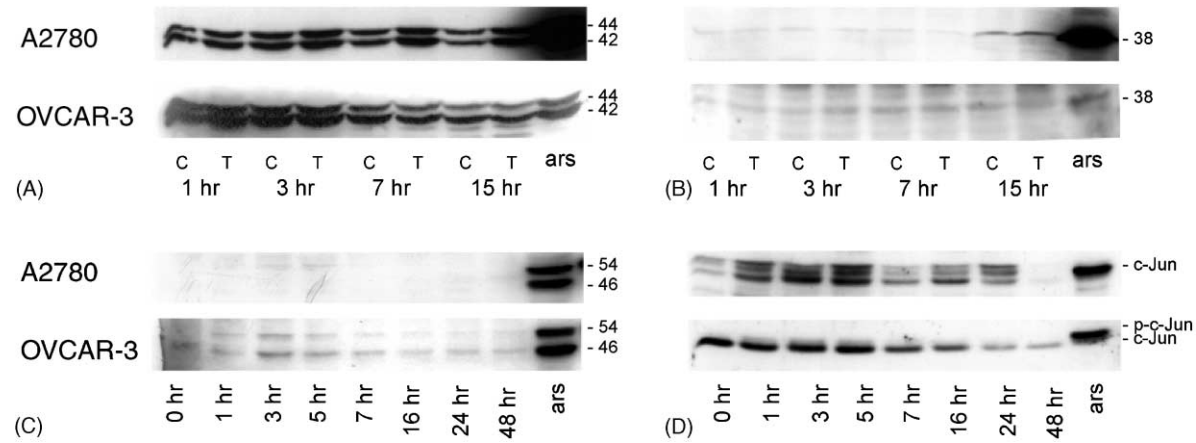

Fig. 5. Phosphorylated ERK1/2, p38, JNK1/2 and c-Jun levels in A2780 and OVCAR-3. Protein samples (50 μg) were analyzed by Western blot. Cells treated with arsenite (ars) were included as a positive control. (A) Phosphorylated ERK1/2 levels and (B) phosphorylated p38 levels. Cells were either control (C) or treated with the IC_{90} concentration of docetaxel (T) for 1 hr. Cells were harvested at 1, 3, 7 and 15 hr after drug exposure. (C) Phosphorylated JNK1/2 levels and (D) total c-Jun and phosphorylated c-Jun in cells treated with the IC_{90} concentration of docetaxel for 1 hr. Cells were harvested at 0, 1, 3, 5, 7, 16, 24 and 48 hr after the start of the 1 hr drug exposure.

similar in time when compared to the levels in control cells (Fig. 5B). Phosphorylated p38 was not detectable in H134 and IGROV-1 before treatment, which did not change upon treatment. Total levels of p38 were unaffected in H134, IGROV-1 and OVCAR-3, but increased in control and treated A2780 cells.

Phosphorylated JNK1/2 was not detectable in A2780 before and after treatment with docetaxel (Fig. 5C). In H134 and IGROV-1, the expression levels of phosphorylated JNK1/2 were low and did hardly change upon treatment. In OVCAR-3 the expression levels of phosphorylated JNK1/2 were also low and did not change in the control samples. A slight increase in phosphorylated JNK1/2, however, was detectable 1 hr after treatment, which reached a maximum after 3 hr and decreased thereafter (Fig. 5C). The levels of total JNK1/2 did not change upon treatment in all experiments.

The positive control drug arsenite showed clear phosphorylation of ERK1/2, p38 and JNK1/2 (Fig. 5A–C). We did, however, not observe Bcl-2 phosphorylation upon treatment with 100 μM arsenite, while OVCAR-3 clearly showed a phosphorylated band of Bcl-2.

Phosphorylated ERK1/2 may contribute to the sensitivity of A2780 to docetaxel, since this is the only cell line which shows changes in phosphorylated ERK1/2 levels. It is unlikely for JNK1/2 that this protein is of major influence on Bcl-2 phosphorylation or apoptosis, since JNK1/2 phosphorylation is only detectable in OVCAR-3.

3.8. c-Jun phosphorylation

To determine if the phosphorylation of JNK1/2 was sufficient to further phosphorylate substrates we investigated this process in OVCAR-3 cells (Fig. 5D). Phosphorylation of c-Jun was detectable at 1 hr, reaching a maximum at 5 hr. At later time-points c-Jun phosphorylation decreased and was no longer detectable at 48 hr. Total levels of c-Jun also decreased in time and the mobility shift of phosphorylated c-Jun disappeared. No phosphorylation of c-Jun could be detected in the other cell lines (data not shown).

Phosphorylated JNK1/2 in OVCAR-3 is able to phosphorylate its substrate c-Jun. The role of phosphorylated JNK1/2 in apoptosis, however, is not established.

4. Discussion

As most studies have focused on paclitaxel, we considered docetaxel of interest in its role to induce apoptosis in human ovarian cancer cells. Ovarian cancer represents a tumor type in which docetaxel is effective. Our experimental design mimicked the clinic, in which patients are usually treated with docetaxel in a 1 hr infusion [1]. The mean C_{max} value of docetaxel is 4.7 μmol/L in patients treated with 100 mg/m^2 which is far higher than the 25–510 nM used in our cell lines. We demonstrated that G2/M arrest followed by apoptosis is a mechanism of docetaxel-induced cell death. When using equitoxic concentrations of docetaxel in four unselected human ovarian cancer cell lines, it was found that A2780 was the most sensitive cell line and had the lowest extent of apoptosis. There was no correlation between the sensitivity of the cells to docetaxel and the apoptotic response.

The behavior of the cells from G2/M arrest to apoptosis upon docetaxel treatment was measured at several time-points up to 96 hr. The use of different time-points is clearly of importance, since the results of the tests varied in time. Already at 8 hr, H134, IGROV-1 and OVCAR-3 showed an accumulation of cells in the G2/M phase of the cell cycle. Preceding DNA degradation and the visualization of condensed nuclei an increase in caspase-3 activity

was evident at 8 hr for OVCAR-3 and at 24 hr for H134 and IGROV-1. The increase in the percentage of apoptosis was detected in H134, IGROV-1 and OVCAR-3 at 48 hr. Overall, the extent of apoptosis in the three cell lines was in line, but the kinetics of this process was different at the time-points measured.

Although the apoptotic patterns for the three cell lines, H134, IGROV-1 and OVCAR-3 were in line, the percentages of apoptosis were dependent on the technique in use. In the case of docetaxel, TUNEL was found to be more reliable than FACS or MGG to measure the extent of apoptosis. First, TUNEL was more sensitive than FACS as the number of cells with DNA fragmentation measured with TUNEL was higher than measured as cells with subG0 DNA content by FACS. An explanation may be that DNA degradation after the mitotic block, in which cells contain a double DNA content, will not all be detectable by FACS. Second, with TUNEL the percentage of apoptotic cells was higher at early time-points than counted with MGG staining of condensed nuclei only. It is likely that DNA degradation precedes the appearance of cells with condensed nuclei.

Docetaxel was able to arrest cells in the G2/M phase of the cell cycle at 8 hr, which was followed by the appearance of cells with multifragmented nuclei at 24 hr. Cells with multifragmented nuclei stained negative with TUNEL at early time-points and, therefore, these cells would not be considered apoptotic according to the test criteria. At later time-points, however, a proportion of cells with fragmented nuclei stained positive for TUNEL. It is likely that cells first are arrested in mitosis, followed by nuclear fragmentation, DNA degradation and subsequent apoptosis. This phenomenon has been described before as the development of an aberrant mitotic exit into a G1-like ''multinucleate state'', which eventually leads to apoptosis [3,8].

The expression levels of p53 and p21/WAF1 increased in all cell lines expressing wt p53. No relation was detected between the p53 status and drug sensitivity or apoptosis induced by docetaxel. It has been described earlier, that paclitaxel and also docetaxel can kill cancer cells in a p53-independent manner [8,14,29]. Moreover, toxicity is more efficient in cells depleted of functional p53 than in those with wt p53 [9]. Indeed, OVCAR-3 (mt p53) showed high levels of apoptosis, but the extent was not much different from that in H134 and IGROV-1 (wt p53). The accumulation of cells in the G2/M-phase of the cell cycle also seems to be p53-independent, since both cells expressing wt p53 and cells expressing mt p53 accumulated in the G2/M phase. Furthermore, the G2/M-arrest is p21/WAF1-independent, as OVCAR-3 did not show an increase in p21/WAF1, while the other two cell lines did. The biochemical events downstream of the G2/M arrest resulting in apoptosis, remain to be investigated.

Except for a slight increase in Bax and Bcl-2 expression levels in OVCAR-3, no changes in Bax or Bcl-2 were observed in the cell lines in which docetaxel clearly induced a G2/M arrest and apoptosis. We demonstrated, as expected, that H134, IGROV-1 and OVCAR-3 cells did show Bcl-2 phosphorylation. It has been described before that drugs affecting microtubule integrity by inhibiting (de)polymerization will cause loss of Bcl-2 anti-apoptotic function through hyperphosphorylation [14]. The duration of Bcl-2 phosphorylation was longer in OVCAR-3 and this was not related to the extent of apoptosis. Furukawa *et al*. [30] have demonstrated as well that phosphorylation was correlated with the accumulation of cells in the G2/M phase and that this was not proportional to the level of apoptosis.

It is not clear whether MAPKs play a role in apoptosis or Bcl-2 phosphorylation as a response to docetaxel. Only in OVCAR-3 cells we measured an activation of JNK1/2, which was sufficient to induce c-Jun phosphorylation. JNK1/2 phosphorylation was already detectable after 1 hr and decreased after 3 hr. Therefore, it seems unlikely that JNK1/2 directly phosphorylates Bcl-2, as this process was maximal at 24 hr. Furthermore, apoptotic characteristics were not detected before 24 hr, which was far later than the induction of JNK1/2 (1 hr) in OVCAR-3 cells. A role for ERK1/2 or p38 in docetaxel-induced apoptosis is also unlikely, as under the experimental conditions no phosphorylation could be detected in any of the cell lines. It seems that the MAPK pathway (JNK1/2, ERK1/2, p38) is not or indirectly involved in Bcl-2 phosphorylation or apoptosis, which is in agreement with the results of Blagosklonny *et al*. [24].

In contrast to the considerable extent of apoptosis in H134, IGROV-1 and OVCAR-3, the percentage of apoptosis was low in A2780 upon treatment with an equitoxic dose of docetaxel. In addition, these cells accumulated in the S-phase, Bcl-2 phosphorylation was absent and caspase-3 activation was extremely low. Of interest, A2780 was the most sensitive cell line and, therefore, it seems that A2780 cells are vulnerable to a different cell death mechanism. It has been recognized that a caspase-independent programmed cell death can occur with necrotic morphology [31,32]. This cell death is negative for TUNEL staining and there is no overall cell condensation. Components of the Fas pathway are now being associated with the ability of cells to die by a necrotic-like morphology [33,34]. Of interest, it has been described in A2780 cells by Henkels and Turchi [35] that cisplatin can induce expression of FADD in A2780 cells without activation of caspase-3 or a considerable extent of apoptosis. Another characteristic of A2780 which may play a role is the very low level of the anti-apoptotic protein Bcl-2 when compared to the levels in the other three cell lines. In contrast, Bax expression levels increased upon docetaxel treatment in A2780 cells. Xiang *et al*. [36] have demonstrated that Bax is able to induce a necrotic-like, caspase-independent cell death. A possible role for FADD in the absence of caspase activation and perhaps also for Bax to explain

non-apoptotic cell death in A2780 remain to be investigated. Considering the latter aspect, other apoptosis-related proteins, such as the anti-apoptotic protein Bcl-X_L, should be measured as well.

Docetaxel-induced apoptosis is remarkably similar to the apoptotic features described for paclitaxel. Kinetics of the apoptotic process are variable among the ovarian cancer cell lines tested. We demonstrated, however, that docetaxel is also able to inhibit cell growth without induction of apoptotic morphology. Of interest, the group of Schimming *et al*. [29] has studied the efficacy of docetaxel in 15 murine tumors *in vivo* and found that neither mitosis nor apoptosis were significantly correlated with tumor growth delay. A recent report of Tannock and Lee [37] further supports the hypothesis that death mechanisms, other than apoptosis play an important role in drug cytotoxicity. Thus, the relevance of non-apoptotic cell death induced by docetaxel should not be underestimated in the treatment of ovarian cancer in the clinic.

References

[1] Eisenhauer EA, Vermorken JB. The taxoids: comparative clinical pharmacology and therapeutic potential. Drugs 1998;55:5–30.

[2] Lavelle F, Bissery MC, Combeau C, Riou JF, Vrignaud P, Andre S. Preclinical evaluation of docetaxel (Taxotere). Semin Oncol 1995; 22:3–16.

[3] Jordan MA, Wendell K, Gardiner S, Derry WB, Copp H, Wilson L. Mitotic block induced in HeLa cells by low concentrations of paclitaxel (Taxol) results in abnormal mitotic exit and apoptotic cell death. Cancer Res 1996;56:816–25.

[4] Lieu CH, Chang YN, Lai YK. Dual cytotoxic mechanisms of submicromolar taxol on human leukemia HL-60 cells. Biochem Pharmacol 1997;53:1587–96.

[5] Blagosklonny MV, Schulte TW, Nguyen P, Mimnaugh EG, Trepel J, Neckers L. Taxol induction of p21WAF1 and p53 requires c-raf-1. Cancer Res 1995;55:4623–6.

[6] Tishler RB, Lamppu DM, Park S, Price BD. Microtubule-active drugs taxol, vinblastine, and nocodazole increase the levels of transcriptionally active p53. Cancer Res 1995;55:6021–5.

[7] Zaffaroni N, Silvestrini R, Orlandi L, Bearzatto A, Gornati D, Villa R. Induction of apoptosis by taxol and cisplatin and effect on cell cycle-related proteins in cisplatin-sensitive and -resistant human ovarian cells. Br J Cancer 1998;77:1378–85.

[8] Woods CM, Zhu J, McQueney PA, Bollag D, Lazarides E. Taxol-induced mitotic block triggers rapid onset of a p53-independent apoptotic pathway. Mol Med 1995;1:506–26.

[9] Wahl AF, Donaldson KL, Fairchild C, Lee FY, Foster SA, Demers GW, Galloway DA. Loss of normal p53 function confers sensitization to Taxol by increasing G2/M arrest and apoptosis. Nat Med 1996;2: 72–9.

[10] Barboule N, Chadebech P, Baldin V, Vidal S, Valette A. Involvement of p21 in mitotic exit after paclitaxel treatment in MCF-7 breast adenocarcinoma cell line. Oncogene 1997;15:2867–75.

[11] Ibrado AM, Kim CN, Bhalla K. Temporal relationship of CDK1 activation and mitotic arrest to cytosolic accumulation of cytochrome *c* and caspase-3 activity during Taxol-induced apoptosis of human AML HL-60 cells. Leukemia 1998;12:1930–6.

[12] Nicholson DW, Ali A, Thornberry NA, Vaillancourt JP, Ding CK, Gallant M, Gareau Y, Griffin PR, Labelle M, Lazebnik YA, Munday NA, Raju SM, Smulson ME, Yamin T-T, Yu VL, Miller DK. Identification and inhibition of the ICE/CED-3 protease necessary for mammalian apoptosis. Nature 1995;376:37–43.

[13] Korsmeyer SJ. BCL-2 gene family and the regulation of programmed cell death. Cancer Res 1999;59:1693s–700s.

[14] Srivastava RK, Srivastava AR, Korsmeyer SJ, Nesterova M, Cho-Chung YS, Longo DL. Involvement of microtubules in the regulation of Bcl2 phosphorylation and apoptosis through cyclic AMP-dependent protein kinase. Mol Cell Biol 1998;18:3509–17.

[15] Haldar S, Basu A, Croce CM. Bcl2 is the guardian of microtubule integrity. Cancer Res 1997;57:229–33.

[16] Scatena CD, Stewart ZA, Mays D, Tang LJ, Keefer CJ, Leach SD, Pietenpol JA. Mitotic phosphorylation of Bcl-2 during normal cell cycle progression and Taxol-induced growth arrest. J Biol Chem 1998;273:30777–84.

[17] Blagosklonny MV, Giannakakou P, El-Deiry WS, Kingston DG, Higgs PI, Neckers L, Fojo T. Raf-1/bcl-2 phosphorylation: a step from microtubule damage to cell death. Cancer Res 1997;57:130–5.

[18] Lee LF, Li G, Templeton DJ, Ting JP. Paclitaxel (Taxol)-induced gene expression and cell death are both mediated by the activation of c-Jun NH2-terminal kinase (JNK/SAPK). J Biol Chem 1998;273: 28253–60.

[19] Wang TH, Popp DM, Wang HS, Saitoh M, Mural JG, Henley DC, Ichijo H, Wimalasena J. Microtubule dysfunction induced by paclitaxel initiates apoptosis through both c-Jun N-terminal kinase (JNK)-dependent and -independent pathways in ovarian cancer cells. J Biol Chem 1999;274:8208–16.

[20] Stone AA, Chambers TC. Microtubule inhibitors elicit differential effects on MAP kinase (JNK, ERK, and p38) signaling pathways in human KB-3 carcinoma cells. Exp Cell Res 2000;254:110–9.

[21] Maundrell K, Antonsson B, Magnenat E, Camps M, Muda M, Chabert C, Gillieron C, Boschert U, Vial-Knecht E, Martinou JC, Arkinstall S. Bcl-2 undergoes phosphorylation by c-Jun N-terminal kinase/stress-activated protein kinases in the presence of the constitutively active GTP-binding protein Rac1. J Biol Chem 1997;272: 25238–42.

[22] Srivastava RK, Mi QS, Hardwick JM, Longo DL. Deletion of the loop region of Bcl-2 completely blocks paclitaxel-induced apoptosis. Proc Natl Acad Sci USA 1999;96:3775–80.

[23] Attalla H, Westberg JA, Andersson LC, Adlercreutz H, Makela TP. 2-Methoxyestradiol-induced phosphorylation of Bcl-2: uncoupling from JNK/SAPK activation. Biochem Biophys Res Commun 1998;247:616–9.

[24] Blagosklonny MV, Chuman Y, Bergan RC, Fojo T. Mitogen-activated protein kinase pathway is dispensable for microtubule-active drug-induced Raf-1/Bcl-2 phosphorylation and apoptosis in leukemia cells. Leukemia 1999;13:1028–36.

[25] De Feudis P, Debernardis D, Beccaglia P, Valenti M, Graniela Sire E, Arzani D, Stanzione S, Parodi S, D'Incalci M, Russo P, Broggini M. DDP-induced cytotoxicity is not influenced by p53 in nine human ovarian cancer cell lines with different p53 status. Br J Cancer 1997;76:474–9.

[26] Gavrieli Y, Sherman Y, Ben-Sasson SA. Identification of programmed cell death *in situ* via specific labeling of nuclear DNA fragmentation. J Cell Biol 1992;119:493–501.

[27] Blom WM, De Bont HJ, Meijerman I, Mulder GJ, Nagelkerke JF. Prevention of cycloheximide-induced apoptosis in hepatocytes by adenosine and by caspase inhibitors. Biochem Pharmacol 1999;58: 1891–8.

[28] Cavigelli M, Li WW, Lin A, Su B, Yoshioka K, Karin M. The tumor promoter arsenite stimulates AP-1 activity by inhibiting a JNK phosphatase. 3 J 1996;15:6269–79.

[29] Schimming R, Mason KA, Hunter N, Weil M, Kishi K, Milas L. Lack of correlation between mitotic arrest or apoptosis and antitumor effect of docetaxel. Cancer Chemother Pharmacol 1999;43:165–72.

[30] Furukawa Y, Iwase S, Kikuchi J, Terui Y, Nakamura M, Yamada H, Kano Y, Matsuda M. Phosphorylation of Bcl-2 protein by CDC2

kinase during G2/M phases and its role in cell cycle regulation. J Biol Chem 2000;275:21661–7.
[31] Chautan M, Chazal G, Cecconi F, Gruss P, Golstein P. Interdigital cell death can occur through a necrotic and caspase-independent pathway. Curr Biol 1999;9:967–70.
[32] Kitanaka C, Kuchino Y. Caspase-independent programmed cell death with necrotic morphology. Cell Death Differ 1999;6:508–15.
[33] Vercammen D, Brouckaert G, Denecker G, Van de Craen M, Declercq W, Fiers W, Vandenabeele P. Dual signaling of the Fas receptor: initiation of both apoptotic and necrotic cell death pathways. J Exp Med 1998;188:919–30.
[34] Kawahara A, Ohsawa Y, Matsumura H, Uchiyama Y, Nagata S. Caspase-independent cell killing by Fas-associated protein with death domain. J Cell Biol 1998;143:1353–60.
[35] Henkels KM, Turchi JJ. Cisplatin-induced apoptosis proceeds by caspase-3-dependent and -independent pathways in cisplatin-resistant and -sensitive human ovarian cancer cell lines. Cancer Res 1999;59:3077–83.
[36] Xiang J, Chao DT, Korsmeyer SJ. BAX-induced cell death may not require interleukin 1 beta-converting enzyme-like proteases. Proc Natl Acad Sci USA 1996;93:14559–63.
[37] Tannock IF, Lee C. Evidence against apoptosis as a major mechanism for reproductive cell death following treatment of cell lines with anti-cancer drugs. Br J Cancer 2001;84:100–5.